

XYLEM VESSEL RELAYS CONTRIBUTE TO RADIAL CONNECTIVITY IN GRAPEVINE STEMS (*VITIS VINIFERA* AND *V. ARIZONICA*; VITACEAE)¹

CRAIG R. BRODERSEN², BRENDAN CHOAT³, DAVID S. CHATELET⁴, KENNETH A. SHACKEL⁵, MARK A. MATTHEWS⁶, AND ANDREW J. McELRONE^{6,7,8}

²Department of Horticultural Science, Citrus Research & Education Center, University of Florida, Lake Alfred, FL 33850

³University of Western Sydney, Hawkesbury Institute for the Environment, Richmond, Australia NSW 2753; ⁴Department of Ecology & Evolutionary Biology, Brown University, Providence, Rhode Island 02912 USA; ⁵Department of Plant Science, University of California, Davis, California 95616 USA; ⁶Department of Viticulture & Enology, University of California, Davis, California 95616 USA and ⁷USDA-ARS, Crops Pathology and Genetics Research Unit, Davis, California 95616 USA

- **Premise of the study:** Xylem network connections play an important role in water and nutrient transport in plants, but also facilitate the spread of air embolisms and xylem-dwelling pathogens. This study describes the structure and function of vessel relays found in grapevine xylem that form radial and tangential connections between spatially discrete vessels.
- **Methods:** We used high-resolution computed tomography, light microscopy, scanning electron microscopy, and single-vessel dye injections to characterize vessel relays in stems and compare their distributions and structure in two *Vitis* species.
- **Key results:** Vessel relays were composed of 1–8 narrow diameter (~25 µm) vessel elements and were oriented radially, connecting vessels via scalariform pitting within a xylem sector delineated by rays. The functional connectedness of vessels linked by vessel relays was confirmed with single-vessel dye injections. In 4.5-cm sections of stem tissue, there were 26% more vessel relays in *V. vinifera* compared with *V. arizonica*.
- **Conclusions:** Because of their spatial distribution within *Vitis* xylem, vessel relays increase the connectivity between vessels that would otherwise remain isolated. Differences in vessel relays between *Vitis* species suggest these anatomical features could contribute to disease and embolism resistance in some species.

Key words: embolism; grapevine; high-resolution computed tomography; HRCT; hydraulic transport; microtomography; vascular pathogens; vessels; water; xylem.

Intervessel connections are a primary determinant of xylem network connectivity (Fujii et al., 2001; Tyree and Zimmermann, 2002; Taneda and Tateno, 2007; Carlquist, 2009), and reconstructions of secondary xylem from transverse serial sections have revealed complex radial, tangential, and axial transport pathways to move water over long distances (Bosshard and Kucera, 1973; Tyree and Zimmermann, 2002; Kitin et al., 2004, 2009). However, the propensity for the spread of both embolisms and xylem-dwelling pathogens is also necessarily dependent on the extent of vessel-to-vessel connectivity, and xylem organization is representative of a balance between safe and efficient water transport (Tyree and Zimmermann, 2002).

Recent research has broadened our understanding of xylem networks by employing high-resolution computed tomography (HRCT) as a nondestructive x-ray-based imaging tool to visualize xylem structure in wood (Steppe et al., 2004; Mannes et al., 2010; Mayo et al., 2010). HRCT combined with commercial and custom visualization and analytical software has revealed the three-dimensional (3D) organization of vessel networks in grapevine (*Vitis vinifera*), including the spatial orientation and distribution of vessel-to-vessel connections (Brodersen et al., 2011), leading to a better understanding the structure–function relationships of xylem networks.

Our recent analysis of the xylem network in grapevine stems showed that intervessel connectivity is highly dependent upon the proximity of large-diameter, adjacent vessels (Brodersen et al., 2011). In the course of this work, HRCT image analysis also revealed conspicuous radial chains of short (axially), narrow diameter vessel elements connecting larger diameter vessels that otherwise lack any apparent direct connections (i.e., shared walls). Although functionally similar anatomical structures have been characterized in the primary xylem of monocot stems (e.g., “bridges”, Tyree and Zimmermann, 2002), to our knowledge, this anatomical feature (hereafter referred to as vessel relays) remains without structural and functional 3D description in the secondary xylem of dicotyledonous plants.

The goal of this study was to characterize the anatomy, spatial distribution, and function of vessel relays and to compare their distribution and structure in xylem networks of two grapevine species (*V. vinifera* and *V. arizonica*). *Vitis vinifera*, a liana, has long and wide vessels, and compared with most woody plants,

¹Manuscript received 23 December 2011; revision accepted 19 November 2012.

The authors thank A. MacDowell and D. Parkinson of beamline 8.3.2 at the Lawrence Berkeley National Laboratory Advanced Light Source for technical assistance, A. Walker for providing grapevine material, and L. Jordan, J. Shogren, and K. Zhao for data collection and analysis. They also thank S. Jansen for helpful comments and S. Carlquist for a careful critique that significantly improved the clarity of the manuscript. This work was supported by a National Science Foundation grant (0818479) and USDA-ARS CRIS funding (Research Project 5306-21220-004-00). The Advanced Light Source is supported by the Director, Office of Science, Office of Basic Energy Sciences, of the U. S. Department of Energy under contract no. DE-AC02-05CH11231.

⁸Author for correspondence (e-mail: ajmcelrone@ucdavis.edu)

doi:10.3732/ajb.1100606

its xylem network is relatively susceptible to cavitation and embolism (Choat et al., 2010; Maherali et al., 2004). *Vitis vinifera* is also susceptible to xylem-dwelling pathogens such as *Xylella fastidiosa* (Xf), that causes Pierce's disease (PD) (Hopkins and Purcell, 2002). Subspecies of *X. fastidiosa* also affect citrus, almonds, peaches, blueberry, coffee, and oleander (Hopkins, 1989), yet most plant species are asymptomatic alternative *Xylella* hosts (Chatelet et al., 2011). Indeed, *V. arizonica*, a grapevine species native to the arid regions of the southwestern United States and northern Mexico is resistant to Xf. Riaz et al. (2008) suggested that an as yet unidentified anatomical difference between *V. vinifera* and *V. arizonica* may play a role in their differential resistance to PD, but a specific disease resistance mechanism has yet to be confirmed. Vessel relays could play an important role in xylem network connectedness and the distribution of water, nutrients, air embolisms, and pathogens throughout plants.

MATERIALS AND METHODS

Plant material—Grapevine plants (*Vitis vinifera* L. cv. Chardonnay and *Vitis arizonica* Engelm.) were grown in a greenhouse on the University of California, Davis campus from rooted cuttings planted in 14-L pots filled with a 1/3 peat, 1/3 sand, 1/3 composted fir bark soil mixture with 2.04 kg dolomite/m³. Plants were irrigated three times daily with half-strength Hoagland solution and supplied with supplemental lighting on a 16 h day/8 h night cycle.

Serial sectioning and light microscopy—Mature stem internodes without defect were cut into 5-cm segments and preserved in 70% ethanol. Several hours before sectioning, the stem segments were soaked in water to soften the tissues. The segments were sectioned in the transverse plane at a thickness of

50 μ m using a sliding microtome (AO-860, American Optical, Buffalo, New York, USA). Every 100 μ m, a section was collected (i.e., discarding every second section) and stained with 0.1% (w/v) aqueous toluidine blue O for 25 s. The sections were then mounted in order and covered with a coverslip and 1:1 glycerin and ethanol solution. Each section was photographed with a Pixera 600ES digital camera (Pixera, Los Gatos, California, USA) mounted on an Olympus Vanox-AHBT (Olympus America, Melville, New York, USA) compound light microscope. All sections were photographed using a 10 \times objective to observe the occurrence of vessel relays between vessels along the axial length of the stem.

High-resolution computed tomography—Internode sections of *V. vinifera* and *V. arizonica* 4.5 cm long were cut from greenhouse-grown plants of the same age and dried at 40°C for 24 h in a drying oven before scanning at the x-ray microtomography facility, beamline 8.3.2, at the Lawrence Berkeley National Laboratory Advanced Light Source, following the methods of Brodersen et al. (2011). Briefly, a section of stem was rotated in the 5 \times 10 mm field of view in 0.125° increments around 180° in a 15 keV x-ray beam, yielding 1440 two-dimensional (2D) projection images per sample, with a voxel (volumetric pixel element) size of 4.5 μ m. The sample was then advanced vertically and repeatedly scanned to create a seamless 4.5-cm long data set. The images were then normalized using a filtered back projection algorithm (Dierick et al., 2004). Normalized 2D images were reconstructed using Octopus 8.3 software (Institute for Nuclear Sciences, University of Ghent, Belgium) to create a 3D, 16-bit series or stack of tagged image file (TIF) format files. Each TIF image was composed of 3D voxels, where voxel intensity was based on x-ray attenuation. Each voxel was then assigned an x, y, and z coordinate in 3D space. Images were processed with an edge-preserving filter in Avizo 6.2 software (VSG, Burlington, Massachusetts, USA) to increase contrast between plant tissue and vessel lumen.

Vessel relays were identified by scrolling through the stacks of transverse image slices within the 4.5 cm long 3D data sets. The Avizo visualization software allowed for virtual slices in any orientation to be displayed such that longitudinal planes could be visualized that bisected each vessel relay. The number of vessel relay cells linking two large-diameter vessels was determined by

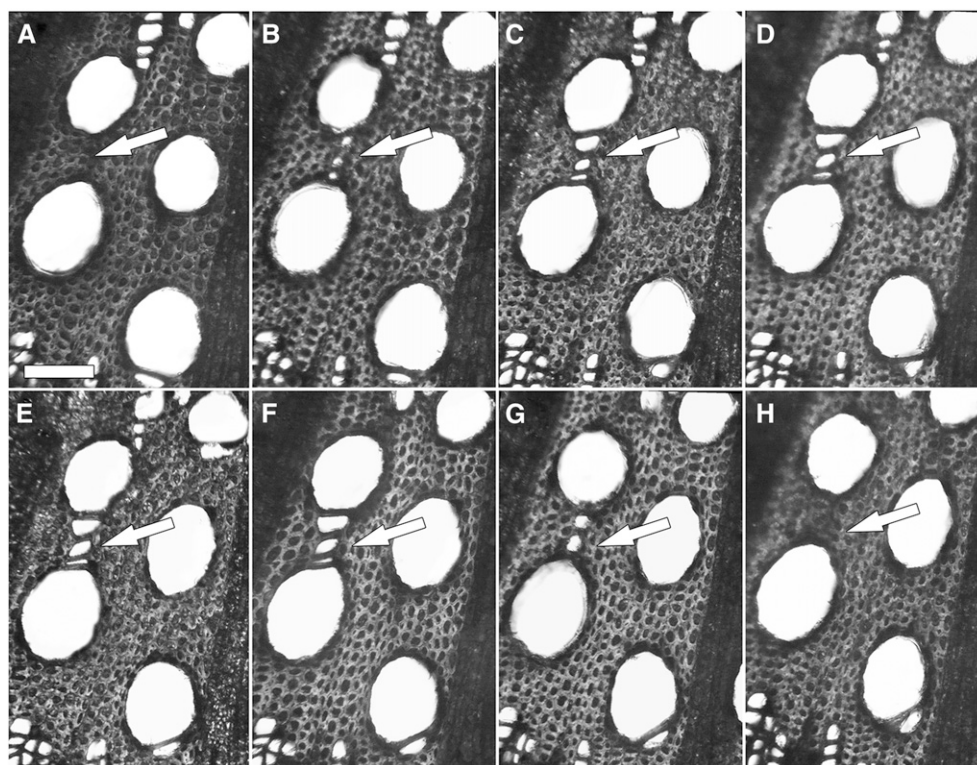


Fig. 1. Light micrographs of serial transverse sections (100 μ m apart) through the length of a *Vitis vinifera* internode (A–H) revealing the location of a conductive xylem vessel relay (arrow) linking two large-diameter vessels. The region above and below the vessel relay cells along the axis consists of parenchyma cells and fibers. Bar = 75 μ m.

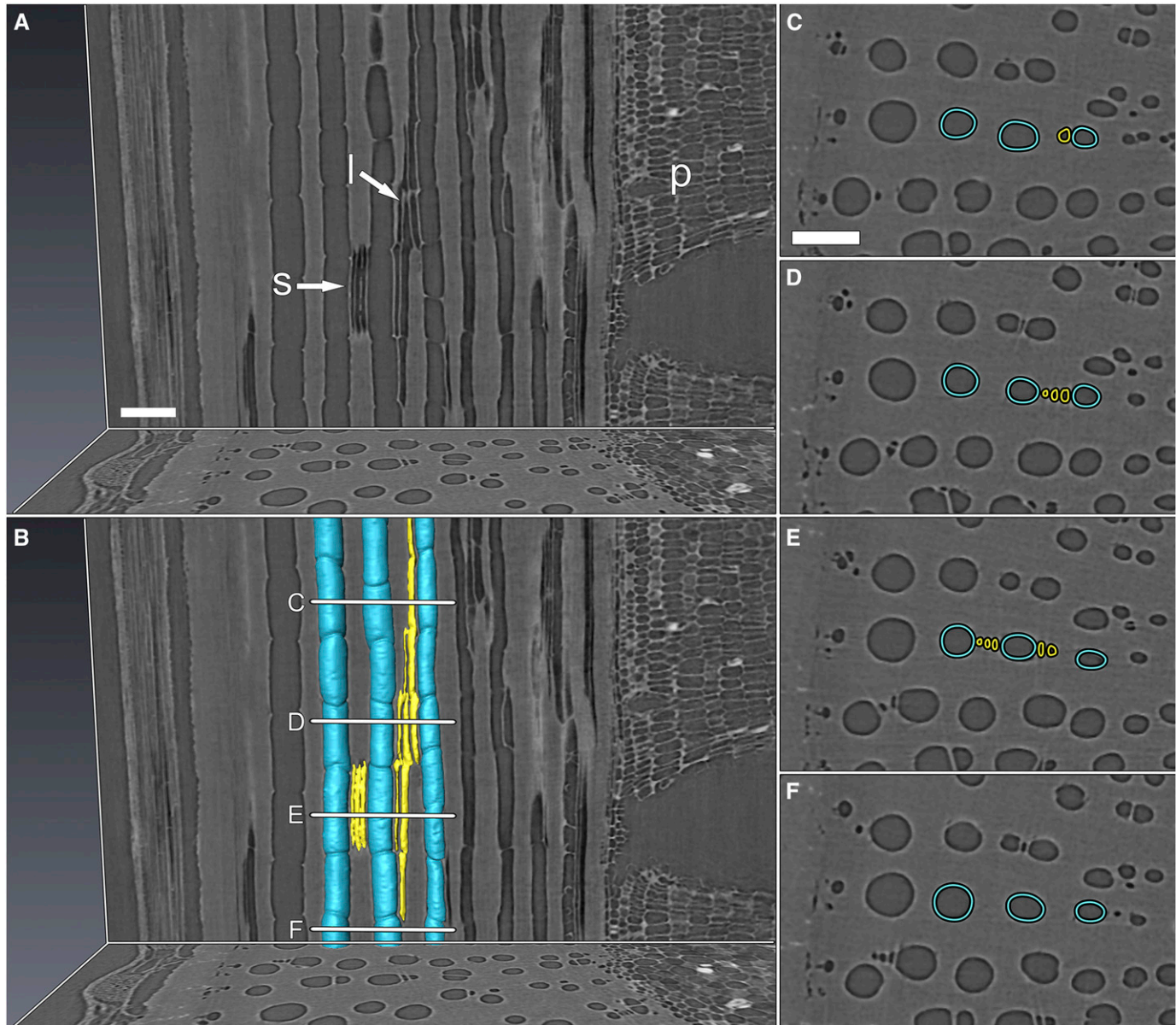


Fig. 2. (A) Longitudinal and transverse high-resolution computed tomography (HRCT) micrographs and (B) 3D volume renderings showing both short and long vessel relay types connecting large-diameter vessels within the same radial sector. The pith (p) is to the right of the image. (A) The short vessel relay (s) spans a single vessel element, while the long vessel relay (l) spans six vessel elements. (B) A 3D volume rendering of the vessels (blue) and vessel relay (yellow). Lines C to F correspond to the respective transverse HRCT images in panels C to F, with vessel outlines in blue and vessel relay outlines in yellow. Here, the short vessel relay is composed of three short elements (B, E), but the long vessel relay is composed of a longer cell file of many more elements. Bars = 250 μ m.

scrolling through the 3D image stack to the axial midpoint of the vessel relay, measuring the distance between the connected large-diameter vessels, and then counting the number of visible vessel relay cells identified in the samples. The x , y , and z coordinates of the axial center of each vessel relay were determined in relation to the center of the stem and the edge of the pith using the PointProbe tool in Avizo. The center of the stem was pinpointed at the intersection of five lines drawn to span the segment diameter to account for the nonsymmetrical perimeter of the stems. The coordinates for the center point were then logged, as well as the position of the pith along the lines bisecting the stem center and the vessel relay. Coordinate data were plotted (see Fig. 5) using the program Sigma Plot 11.0 (Systat Software, San Jose, California, USA).

Scanning electron microscopy—Fresh stem samples were dissected using a stereomicroscope and razor blade to expose transverse or longitudinal sections

of the xylem tissue. Enough samples were dissected to expose 15 vessel relays each from both *V. vinifera* and *V. arizonica*. The samples were then dried at 40°C for 24 h, sputter-coated with gold, and observed at 5 kV with an FEI/Philips XL30-SFEG scanning electron microscope (FEI, Hillsboro, Oregon, USA). SEM micrographs were analyzed visually using ImageJ software (National Institutes of Health, Bethesda, Maryland, USA) to confirm the presence of intervessel scalariform pits and pit membranes between vessels, between vessels and vessel relay cells, and between vessels and parenchyma cells.

Functional connectivity of vessels via conductive xylem vessel relays—To confirm the functional connectivity between vessels via vessel relay cells, empirical measurements were made using the microcapillary technique method of Choat et al. (2006). Briefly, four internode sections of *V. vinifera* stem were cut perpendicular to the stem axis to expose the transverse surface. Next, a

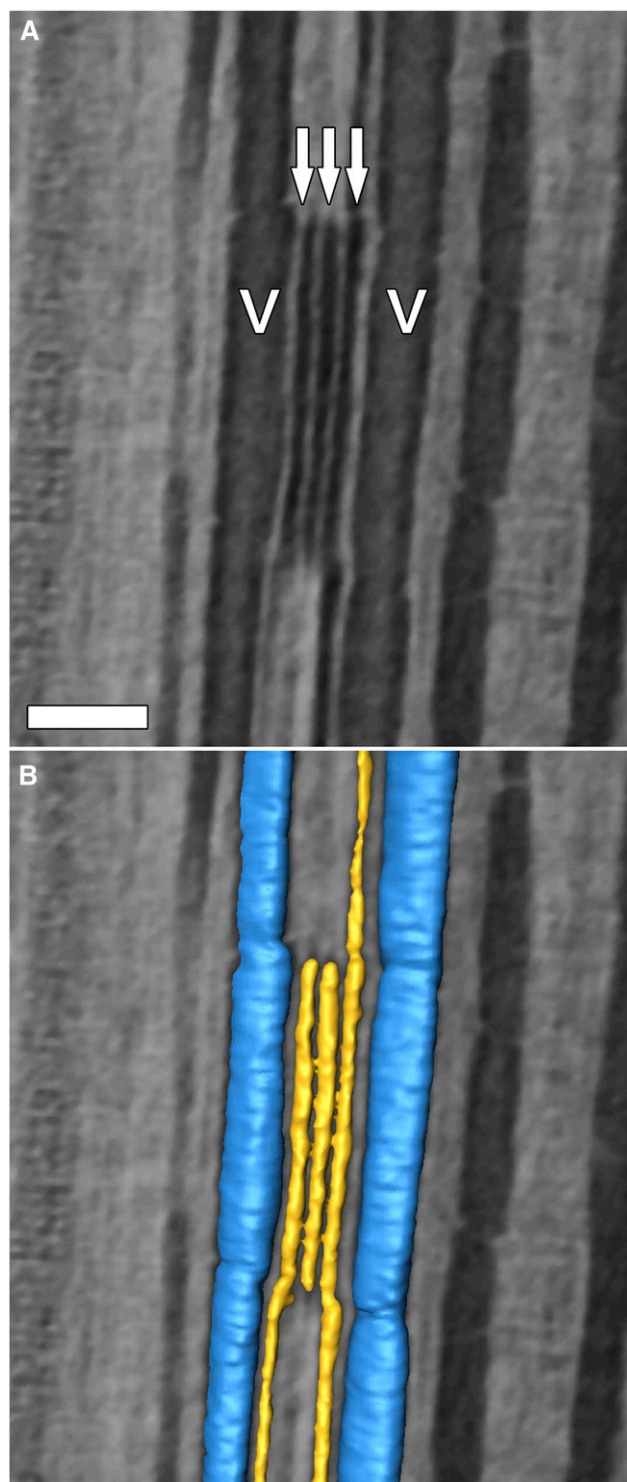


Fig. 3. Longitudinal high-resolution computed tomography (HRCT) micrographs and volume renderings showing a short vessel relay (i.e., one that spans the length of only one vessel element). (A) Longitudinal HRCT section (dark area = vessel lumen, light area = cell walls of parenchyma and fibers) shows two large-diameter vessels (V) connected in the radial direction by a vessel relay consisting of three small diameter conduits (arrows); (B) 3D volume rendering of the same sections shown in panel A illustrates the vessel lumen (blue) shows connectivity through vessel relay cells (yellow). Here the vessel relay spans a single vessel element in the axial dimension. Bar = 100 μm .

microcapillary was pulled to achieve a tip diameter of 50 μm using a vertical micropipette puller (Stoelting Co., Wood Dale, Illinois, USA) and inserted into the proximal end of an open vessel in close proximity to other vessels within the same sector. The entire proximal end was then sealed with cyanoacrylic glue (Loctite 409, Henkle Corp., Rocky Hill, Connecticut, USA). The distal end of the stem section was cut back with a razor blade to expose the vessel openings so that the final section length was 1–2 cm. A filtered (0.22 μm), 0.01% safranin solution (w/v deionized water) was injected into the vessel at low pressure (<5 kPa) to identify its location at the distal end of the section. The vessel filled with dye was then sealed with glue on the distal surface to ensure flow could only proceed across shared walls or vessel relays into surrounding vessels. The microcapillary tube was mounted in a pipette holder (No. 51442, Stoelting Co.) attached to PEEK tubing (0.76 mm inner diameter, Victrex USA, West Conshohocken, Pennsylvania, USA) in a reservoir of 0.01% safranin solution located in a pressure chamber (#3005, Soil Moisture Systems, Goleta, California, USA). The dye solution was forced through the vessel network using an applied pressure of <0.3 MPa until the dye exited the distal end. The stem sample was then sectioned, mounted, and exposed to epi-illumination with an excitation wavelength of 540 nm, and digitally imaged as described already.

RESULTS

Analysis of serial transverse light microscope sections of *Vitis vinifera* stems showed chains of small diameter (<25 μm) vessel elements (xylem vessel relays) spanning the distance (30–300 μm) between large diameter (>75 μm) vessels within vessel sectors delineated by rays (Fig. 1) and occasionally across rays. Above and below the vessel relays in the axial direction, the vessels were clearly separated by fibers and parenchyma (Fig. 1). Longitudinal and transverse HRCT sections confirmed our observations made with serial light micrographs and revealed two different vessel relay types, short (Figs. 2, 3) and long (Fig. 2).

In transverse cross sections, vessel relays were composed of 1–8 radially aligned cells ca. 25 μm in diameter. Short vessel relays ranged in total axial length from 397 to 559 μm , with an average length of 476.7 ± 55.5 (SD) μm ($N = 10$), and consisted of files of individual vessel elements with tapering ends overlapping axially (Fig. 2). Long vessel relays ranged in total axial length from 685 to 3522 μm , with an average length of 1774.4 ± 752.1 μm ($N = 32$), spanning the length of multiple large-diameter vessel elements. Vessel relays had a mean total contact area of 12838 ± 4722.2 μm^2 and 13694 ± 5873 μm^2 at vessel relay–vessel relay junctions and vessel relay–vessel junctions, respectively. HRCT images showed that combined vessel relay cell wall thickness averaged 12.6 ± 1.5 μm ($N = 20$), which is below the recently demonstrated threshold for intervessel pitting for *V. vinifera* (Brodersen et al., 2011). There was a strong linear relationship between the radial number of cells in a vessel relay and the radial distance between the bridged vessels ($r^2 = 0.88$; Fig. 4); vessel relay cell diameters are relatively constant, while cell numbers increase to span increasing distance between distant vessels.

An HRCT analysis of 4.5-cm stem sections for these species revealed 26% more vessel relays in *V. vinifera* compared to *V. arizonica*, with 29 and 23 vessel relays per centimeter of internode tissue for *V. vinifera* and *V. arizonica*, respectively. The vessel relays in both species were predominantly in the radial direction, connecting vessels within the same sector. Single-vessel dye injection experiments demonstrated that the dye solution could travel between spatially separated large-diameter vessels by way of vessel relays, either radially or tangentially (Fig. 5). Dye was observed moving from a group of vessels within

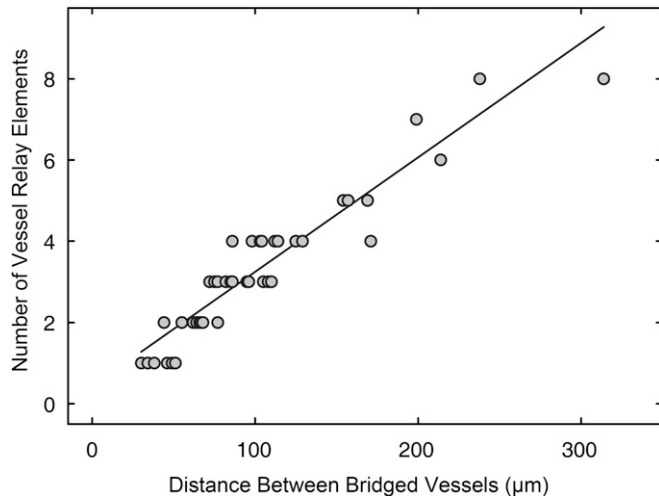


Fig. 4. Linear relationship between the radial distance separating two large-diameter vessels and the number of vessel relay cells spanning that distance in *Vitis vinifera* ($N = 54$, $r^2 = 0.88$). Mean vessel relay cell diameter was $25.1 \mu\text{m}$.

close proximity (i.e., sharing walls), through a series of interconnected vessel relay cells, across ray parenchyma, and into a vessel in a neighboring vessel sector. Only when the vessel relay cells loaded with dye come in contact with the neighboring vessel did dye appear in the large vessel element (Fig. 5). We also found lateral connections, where two vessels separated by a ray were connected through a series of perforated ray cells (data not shown). Most vessel relays were located in the dorsal or ventral secondary xylem sectors of the stem, with fewer vessel relays occurring in the lateral sectors associated with leaves, fruit clusters, or tendrils (Fig. 6).

Scanning electron microscopy revealed that connections within vessel relays in both species were by way of scalariform pit fields (Fig. 7). These pit fields are formed by ladder-like perforations in the secondary walls of adjacent vessels that are separated by pit membranes, which are the remnants of the primary cell walls and middle lamellae (Carlquist, 2001). In one *V. arizonica* vessel relay, we observed simple perforations within the more common scalariform pit fields. This is similar to but clearly different than those found in the lateral walls of adjacent fibriform vessel elements of *Ipomoea arborescens* (Carlquist and Hanson, 1991). Of the 15 *V. vinifera* vessel relays observed with SEM, 67% showed little evidence of pit membranes, and the remaining 33% had either torn or partial remnants of pit membranes (Fig. 7A, B). In the SEM analysis of 15 vessel relays from *V. arizonica* stems, 93% had at least one vessel relay element with intact pit membranes (Fig. 7C, D). In both species nearby vessel-parenchyma and vessel-vessel pit membranes were intact in the same stem sections, but it was not always clear whether damage to the vessel relay pit membranes was due to sample preparation.

DISCUSSION

To our knowledge, this study revealed for the first time the structural and functional relationship of the small diameter vessel elements and the discrete large-diameter vessels to which they connect in grapevine secondary xylem. We term these conductive xylem vessel relays and show that there are radial and tangential connections between the two types of vessels. Previous anatomical

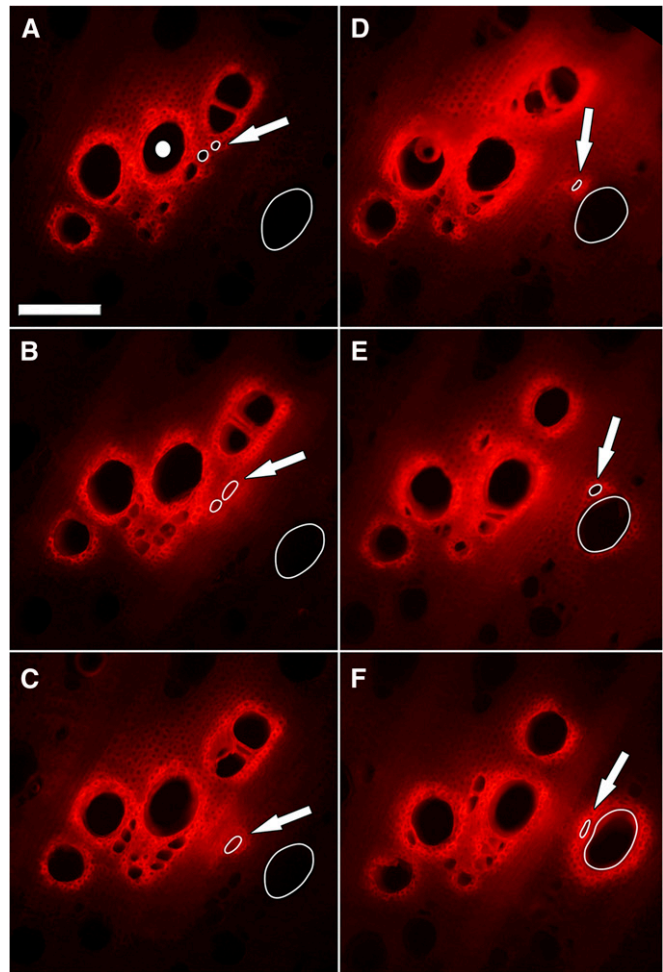
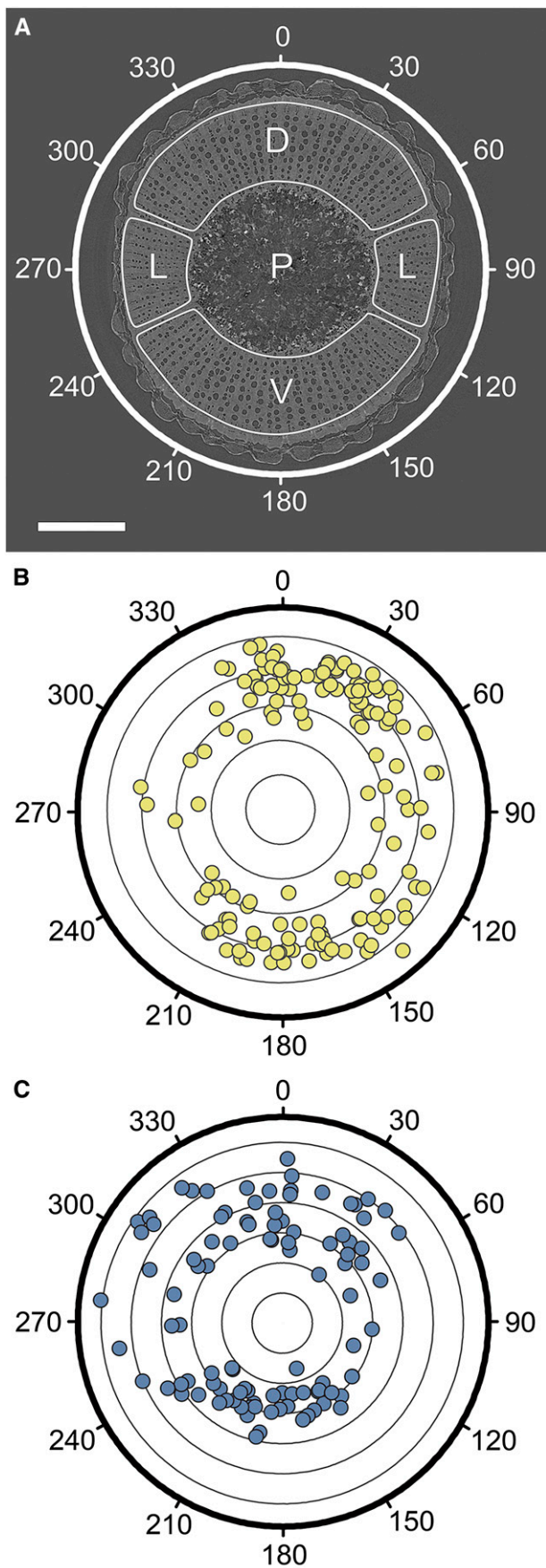


Fig. 5. Tangential movement of safranin dye through a xylem vessel relay. Fluorescence micrographs of transverse serial sections ($200 \mu\text{m}$ apart) through an internode of *Vitis vinifera* (A–F). Safranin dye was injected in a vessel (white dot in A) at low pressure, which flowed via a vessel relay (white outlined vessels) across a ray and into a neighboring vessel. Only when the vessel relay is complete and all elements are filled (E) does the target vessel show evidence of dye. Bar = $150 \mu\text{m}$.

descriptions of xylem networks in grapevine using light microscopy and xylem macerations (e.g., Adkinson, 1913; Pratt, 1974) did not comment on vessel relays nor provide a functional explanation for the narrow diameter elements of xylem structure. When viewed in transverse section, vessel relays appear as a chain of narrow diameter vessel elements bounded by larger diameter vessel elements (i.e., “radial multiples”, Carlquist, 1984; “median band vessels”, Carlquist, 2009). Lengths of these narrow-diameter vessels have been difficult to determine because of the 3D organization of secondary xylem and the nonplanar nature of axial cell files. HRCT imaging, in which longitudinal sections are reconstructed and visualized, removes the ambiguity when viewing this type of structure in 3D (Figs. 1D–F, 2C–F).

The vessel relay cells documented here do not appear to result from abnormal growth or a wounding response that disrupted normal cell differentiation because vessel relay conduits develop simple perforation plates with similar axial spacing to the surrounding vessels, which suggests concurrent development of vessels and vessel relays (Figs. 2, 3) (Jacobs, 1952; Berleth



et al., 2000). Xylem redifferentiation in response to wounding is well documented in *Coleus* spp. and other species, where parenchyma cells form irregularly shaped conduits that do not resemble the vessel relays presented here (Sachs, 1981; Sachs and Cohen, 1982; Aloni and Baum, 1991). Furthermore, vessel relay cells were consistently uniform in diameter as demonstrated by the strong linear relationship between the number of vessel relay cells and the distance between vessels (Fig. 4). These data suggest that vessel relay cells are produced as part of normal cambial activity.

The mechanism responsible for the increased damage to or increased frequency of fragmented *V. vinifera* pit membranes remains unclear. Intervessel pit membranes visualized with SEM in *Vitis* are typically intact (Sun et al., 2011) and limit the movement of air and pathogens between connected vessels while maintaining water transport (Sperry and Hacke, 2004; Choat et al., 2008). Intact *V. vinifera* pit membrane pores are known to be less than 20 nm in diameter (Perez-Donoso et al., 2010) and considerably smaller than the size of an individual *Xf* bacterium. The bacterial cells are known to aggregate in scalariform pits and secrete cell wall degrading enzymes, the putative means of *Xf* spread throughout grapevine xylem networks (Perez-Donoso et al., 2010; Sun et al., 2011). While greenhouse growth conditions and sample preparation were identical for both species in the present study and established protocols for pit membrane SEM visualization were followed (Jansen et al., 2008; Li and Ren, 2011), the shear and torsion stress imposed by sectioning may ultimately have led to pit membrane damage (Carlquist and Schneider, 2004). However, even if damage to vessel relay pit membranes resulted from sample preparation (e.g., Carlquist and Schneider, 2004), it occurred differentially between the species and would suggest interspecific differences in pit membrane structural integrity. Recently, Sun et al. (2011) showed that pit membranes of Pierce's disease (PD) susceptible *V. vinifera* and PD-resistant *V. arizonica* differed in polysaccharide composition and suggested these differences result in structurally weaker and more easily degraded pit membranes for PD-susceptible *V. vinifera*.

The difference in the absolute number of vessel relays (i.e., *V. vinifera* > *V. arizonica* per centimeter of internode) and in potential differences in pit membrane structure between the two species was surprising, and those differences have important implications for the safety and efficiency of water transport in grapevines. The presence of vessel relays increases xylem network connectivity and limits the isolation of large-diameter vessels for both species studied here. This pattern is accentuated in *V. vinifera*, where 26% more vessel relays per centimeter of internode results in greater connectivity and in less resistance to embolism and pathogen spread between vessels. Xylem organization in grapevine may be related to age or location in the plant, and lateral hydraulic connectivity in older

Fig. 6. The spatial distribution of vessel relays in 4.5-cm-long internode segments of grapevine. (A) Grapevine stem secondary xylem consists of dorsal (D), ventral (V), and lateral (L) zones surrounding the pith (P). Vessel relay locations in (B) *Vitis vinifera* and (C) *V. arizonica* compressed into a single transverse plane. Each symbol represents the location of one vessel relay. Concentric rings are spaced 500 and 200 μ m apart in (B) and (C), respectively. Outer ring is the approximate location of the epidermis. 0° and 180° are oriented toward the dorsal and ventral sides of the stem, respectively; 90° and 270° are oriented to the lateral sides of the stem.

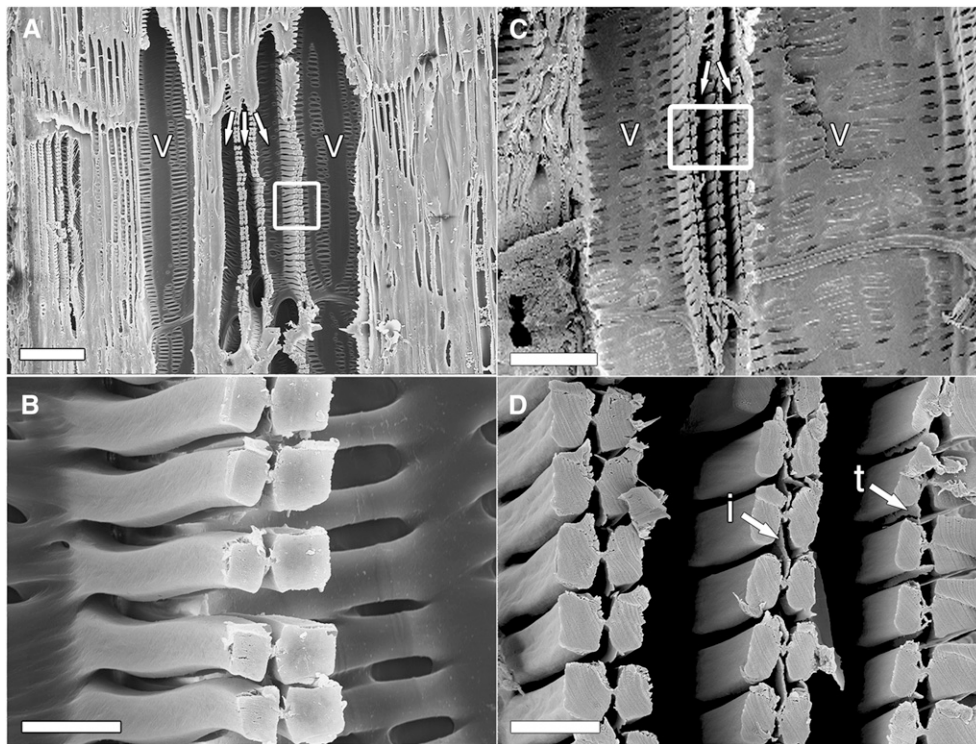


Fig. 7. SEM image of longitudinal section of stems of in (A, B) *V. vinifera* and (C, D) *V. arizonica* showing long vessel relays. (A) Three vessel relay cells (arrows) connect two large-diameter vessels (v). (B) Magnified SEM image of the white box in (A) reveals that pit membrane remnants. Bars = 75 μ m (A), 25 μ m (B). Detail in (B) is representative of the other shared walls in the vessel relay. In (C), two vessel relay cells (arrows) connect two large-diameter *V. arizonica* vessels (v). (D) Magnified SEM image of the area within the white box. Bars = 72 μ m (A), 25 μ m (B), 50 μ m (C), 10 μ m (D).

grapevine wood is frequent and exists primarily through perforated ray cells (Chalk and Chattaway, 1933; Wheeler and LaPasha, 1994; Merev et al., 2005), whereas young grapevine xylem appears to be dominated by radial connections either through vessel relays or direct intervessel connections (Brodersen et al., 2011). For the young stems studied here, the low frequency of lateral vessel relays limits connectivity to a single sector of vessels (i.e., groups of vessels delineated by two rays), and each sector acts as a separate modular unit for water transport.

Vitis vinifera has been cultivated for thousands of years (McGovern, 2000), and in the artificial selection and breeding of varieties suitable for wine and table grape production, viticulturists may have inadvertently selected for a trait (lack of pit membranes in vessel relays or higher frequency of vessel relays) that may make *V. vinifera* more susceptible to both water-stress induced embolism and disease. An alternative explanation is that *V. vinifera* may have had minimal exposure to *Xf* while in its native habitat prior to human cultivation. *Vitis arizonica* is known to be resistant to PD and has been used in breeding programs to confer PD resistance in *V. vinifera* (Krivanek et al., 2005; Fritsch et al., 2007). While the primary mechanism for resistance to PD in *V. arizonica* is still unclear, the presence of fewer vessel relays in the xylem could limit the spread of *Xf* and prevent systemic spread, particularly in light of new research showing structural differences in the pit membranes of these two species (Sun et al., 2011).

LITERATURE CITED

- ADKINSON, J. 1913. Some features of the anatomy of the Vitaceae. *Annals of Botany* 27: 133–139.
- ALONI, R., AND S. F. BAUM. 1991. Naturally occurring regenerative differentiation of xylem around adventitious roots in *Luffa cylindrica* seedlings. *Annals of Botany* 67: 379–382.
- BERLETH, T., J. MATTSSON, AND C. S. HARDTKE. 2000. Vascular continuity and auxin signals. *Trends in Plant Science* 5: 387–393.
- BOSSHARD, H., AND L. KUCERA. 1973. Die dreidimensionale struktur-analyse des holzes—Erste mitteilung: die vernetzung des gefäßsystems in *Fagus sylvatica* L. *Holz Roh-u Werkstoff* 31: 437–445.
- BRODERSEN, C. R., E. F. LEE, B. CHOAT, S. JANSEN, R. J. PHILLIPS, K. A. SHACKEL, A. J. McELRONE, ET AL. 2011. Automated analysis of three-dimensional xylem networks using high resolution computed tomography. *New Phytologist* 191: 1168–1179.
- CARLQUIST, S. 1984. Vessel grouping in dicotyledon wood: Significance and relationship to imperforate tracheary elements. *Aliso* 10: 505–525.
- CARLQUIST, S. 2001. Comparative wood anatomy: Systematic, ecological and evolutionary aspects of dicotyledon wood. Springer-Verlag, Berlin, Germany.
- CARLQUIST, S. 2009. Non-random vessel distribution in woods: Patterns, modes, diversity, correlations. *Aliso* 27: 39–58.
- CARLQUIST, S., AND M. A. HANSON. 1991. Wood and stem anatomy of *Convolvulaceae*: A survey. *Aliso* 13: 51–94.
- CARLQUIST, S., AND E. L. SCHNEIDER. 2004. Pit membrane remnants in perforation plates of Hydrangeales with comments on pit membrane remnant occurrence, physiological significance and phylogenetic distribution in dicotyledons. *Botanical Journal of the Linnean Society* 146: 41–51.
- CHALK, L., AND M. M. CHATTAWAY. 1933. Perforated ray cells. *Proceedings of the Royal Society of London* 113: 82–92.

- CHATELET, D., C. WISTROM, A. PURCELL, T. ROST, AND M. MATTHEWS. 2011. Xylem structure of four grape varieties and twelve alternative hosts to the xylem-limited bacterium *Xylella fastidiosa*. *Annals of Botany* 108: 73–85.
- CHOAT, B., T. W. BRODIE, A. R. COBB, M. A. ZWIENIECKI, AND N. M. HOLBROOK. 2006. Direct measurements of intervessel pit membrane hydraulic resistance in two angiosperm tree species. *American Journal of Botany* 93: 993–1000.
- CHOAT, B., A. R. COBB, AND S. JANSEN. 2008. Structure and function of bordered pits: New discoveries and impacts on whole plant hydraulic function. *New Phytologist* 177: 608–625.
- CHOAT, B., W. DRAYTON, C. BRODERSEN, M. MATTHEWS, K. SHACKEL, H. WADA, AND A. MCELDRONE. 2010. Measurement of the vulnerability to water-stress induced cavitation in grapevine: A comparison of four techniques applied to a long-vesselled species. *Plant, Cell & Environment* 33: 1502–1512.
- DIERICK, M., B. MASSCHAELE, AND L. VAN HOOREBEKE. 2004. Octopus, a fast and user-friendly tomographic reconstruction package developed in LabView®. *Measurement Science & Technology* 15: 1366–1370.
- FRITSCHI, F. B., H. LIN, AND M. A. WALKER. 2007. *Xylella fastidiosa* population dynamics in grapevine genotypes differing in susceptibility to Pierce's disease. *American Journal of Enology and Viticulture* 58: 326–332.
- FUJII, T., S. J. LEE, N. KURODA, AND Y. SUZUKI. 2001. Conductive function of intervessel pits through a growth ring boundary of *Machilus thunbergii*. *International Association of Wood Anatomists Journal* 22: 1–14.
- HOPKINS, D. L. 1989. *Xylella fastidiosa*: Xylem-limited bacterial pathogen of plants. *Annual Review of Phytopathology* 27: 271–290.
- HOPKINS, D. L., AND A. H. PURCELL. 2002. *Xylella fastidiosa*: Cause of Pierce's disease of grapevine and other emergent diseases. *Plant Disease* 86: 1056–1066.
- JACOBS, W. P. 1952. The role of auxin in differentiation of xylem around a wound. *American Journal of Botany* 39: 301–309.
- JANSEN, S., A. PLETTERS, AND Y. SANO. 2008. The effect of preparation techniques on SEM-imaging of pit membranes. *International Association of Wood Anatomists Journal* 29: 161–178.
- KITIN, P. B., T. FUJII, H. ABE, AND R. FUNADA. 2004. Anatomy of the vessel network within and between tree rings of *Fraxinus lanuginosa* (Oleaceae). *American Journal of Botany* 91: 779–788.
- KITIN, P. B., T. FUJII, H. ABE, AND R. FUNADA. 2009. Anatomical features that facilitate radial flow across growth rings and from xylem to cambium in *Cryptomeria japonica*. *Annals of Botany* 103: 1145–1157.
- KRIVANEK, A. F., T. R. FAMULA, A. TENSCHER, AND M. A. WALKER. 2005. Inheritance of resistance to *Xylella fastidiosa* within a *Vitis rupestris* × *Vitis arizonica* hybrid population. *Theoretical and Applied Genetics* 111: 110–119.
- LI, H., AND Y. REN. 2011. The effect of SEM preparation on pit membrane remnants in vessel element end walls of primitive angiosperms. *Flora* 206: 310–315.
- MAHERALI, H. M., W. T. POCKMAN, AND R. B. JACKSON. 2004. Adaptive variation in the vulnerability of woody plants to xylem cavitation. *Ecology* 85: 2184–2199.
- MANNES, D., F. MARONE, E. LEHMANN, M. STAMPANONI, AND P. NIEMZ. 2010. Application areas of synchrotron radiation tomographic microscopy for wood research. *Wood Science and Technology* 44: 67–84.
- MAYO, S. C., F. CHEN, AND R. EVANS. 2010. Micron-scale 3D imaging of wood and plant microstructure using high-resolution x-ray phase-contrast microtomography. *Journal of Structural Biology* 171: 182–188.
- MCGOVERN, P. E. 2000. The origins and ancient history of wine. Gordon and Breach, New York, New York, USA.
- MEREV, N., Z. GERÇEK, AND B. SERDAR. 2005. Wood anatomy of some Turkish plants with special reference to perforated ray cells. *Turkish Journal of Botany* 29: 269–281.
- PÉREZ-DONOSO, A. G., Q. SUN, M. C. ROPER, L. C. GREVE, B. KIRKPATRICK, AND J. M. LABAVITCH. 2010. Cell wall-degrading enzymes enlarge the pore size of intervessel pit membranes in healthy and *Xylella fastidiosa*-infected grapevines. *Plant Physiology* 152: 1748–1759.
- PRATT, C. 1974. Vegetative anatomy of cultivated grapes—A review. *American Journal of Enology and Viticulture* 25: 131–150.
- RIAZ, S., A. C. TENSCHER, J. RUBIN, R. GRAZIANI, S. S. PAO, AND M. A. WALKER. 2008. Fine-scale genetic mapping of two Pierce's disease resistance loci and a major segregation distortion region on chromosome 14 of grape. *Theoretical and Applied Genetics* 117: 671–681.
- SACHS, T. 1981. The control of the patterned differentiation of vascular tissues. *Advances in Botanical Research* 9: 151–262.
- SACHS, T., AND D. COHEN. 1982. Circular vessels and the control of vascular differentiation in plants. *Differentiation* 21: 22–26.
- SPEERY, J. S., AND U. G. HACKE. 2004. Analysis of circular bordered pit function I. Angiosperm vessels with homogeneous pit membranes. *American Journal of Botany* 91: 369–385.
- STEPPE, K., V. CNUDE, C. GIRARD, R. LEMEUR, J. P. CNUDE, AND P. JACOBS. 2004. Use of X-ray computed microtomography for non-invasive determination of wood anatomical characteristics. *Journal of Structural Biology* 148: 11–21.
- SUN, Q., L. C. GREVE, AND J. M. LABAVITCH. 2011. Polysaccharide composition of intervessel pit membranes contribute to Pierce's disease resistance of grapevines. *Plant Physiology* 155: 1976–1987.
- TANEDA, H., AND M. TATENO. 2007. Effects of transverse movement of water in xylem on patterns of water transport within current-year shoots of kudzu vine, *Pueraria lobata*. *Functional Ecology* 21: 226–234.
- TYREE, M., AND M. ZIMMERMANN. 2002. Xylem structure and the ascent of sap. Springer Verlag, Berlin, Germany.
- WHEELER, E. A., AND C. A. LAPASHA. 1994. Woods of the Vitaceae—Fossil and modern. *Review of Palaeobotany and Palynology* 80: 175–207.